Journal of Power Sources 196 (2011) 9130–9140

Contents lists available at ScienceDirect

Journal of Power Sources

journal homepage: www.elsevier.com/locate/jpowsour

Chemical durability of Solid Oxide Fuel Cells: Influence of impurities on long-term performance

Kazunari Sasaki[a,b,c,*], Kengo Haga[a], Tomoo Yoshizumi[a], Daisuke Minematsu[a], Eiji Yuki[a], RunRu Liu[a], Chie Uryu[b], Toshihiro Oshima[a], Teppei Ogura[c], Yusuke Shiratori[a], Kohei Ito[a,b], Michihisa Koyama[c], Katsumi Yokomoto[d]

[a] Kyushu University, Faculty of Engineering, Department of Hydrogen Energy Systems, Motooka 744, Nishi-ku, Fukuoka 819-0395, Japan
[b] Kyushu University, International Research Center for Hydrogen Energy, Motooka 744, Nishi-ku, Fukuoka 819-0395, Japan
[c] Kyushu University, Inamori Frontier Research Center, Motooka 744, Nishi-ku, Fukuoka 819-0395, Japan
[d] Kyushu University, Office for the Promotion of Safety and Health, Motooka 744, Nishi-ku, Fukuoka 819-0395, Japan

ARTICLE INFO

Article history:
Received 26 June 2010
Received in revised form 23 August 2010
Accepted 10 September 2010
Available online 28 June 2011

Keywords:
SOFC
Poisoning
Impurity
Degradation
Anode
Cathode

ABSTRACT

Because of the fuel flexibility of Solid Oxide Fuel Cells (SOFCs), various types of fuels may be applied directly or via a simple reforming process, including hydrocarbons, alcohols, coal gas, biogas, besides hydrogen. However, various types of minor constituents in practical fuels and/or from the system components can cause chemical degradation of SOFCs, such as anode and cathode poisoning phenomena. In this study, we compare the influence of various external impurities, including sulfur, chlorine, phosphorus, boron, and siloxane for anodes, and H_2O and SO_2 for cathodes, on SOFC performance to have a general overview on long-term chemical durability of SOFCs. Chemical compatibility of Ni with foreign species has also been thermochemically considered. Using common model cells, the stability of cell voltage, electrode overpotential, and ohmic loss up to 3000 h has been experimentally examined for H_2-based fuels, for hydrocarbon-based fuels, and for partially pre-reformed CH_4-based fuels. Increase in degradation rate by impurities was verified for various operational parameters. Impurity poisoning mechanisms are discussed for each specific impurity.

1. Introduction

Solid Oxide Fuel Cells (SOFCs) can be regarded as the most flexible fuel cells with respect to fuel selections, so that the use of various types of fuels has been considered [1,2]. Practical fuels, however, contain minor constituents as impurities. In addition, due to a relatively high operational temperature of SOFCs, impurities with a high vapor pressure can also be evaporated from their system components, causing contamination of the SOFC systems. As illustrated in Fig. 1, such extrinsic impurities can cause chemical degradation of SOFCs, as reported, e.g. for sulfur [3–9] and other impurities [10,11]. In fact, as reported by Yokokawa et al. [12], it has been confirmed that various impurities do exist in SOFC systems. In addition, the use of inexpensive system components and raw materials with lower purity may cause impurity poisoning of SOFC systems. Poisoning effects by external contaminants should be taken into account also for the SOFC cathodes because ambient air is continuously supplied directly to the cathodes during operation up to a decade. In the present study, chemical degradation of SOFCs is therefore considered based on thermochemical calculations, long-term poisoning tests up to 3000 h, and microstructural observations, using common model cells for comparison.

2. Thermochemical consideration

Thermochemical calculations are useful to derive the equilibrium compositions of fuels and the stability diagrams with impurities in the SOFC operational temperature range. Such calculations for sulfur compounds have been revealed that H_2S is the most stable sulfur-based compound in the SOFC anode environment [13]. The equilibrium concentrations of other sulfur compounds, such as COS and CH_3SH are negligibly low assuming thermochemical equilibria.

In addition, the reactivity of impurities with SOFC component materials can dominate their chemical degradation. In order to know the reactivity of impurities with Ni anodes, stability diagrams of C–H–O–Ni–X systems and Ni–H–O–X systems have been thermochemically calculated where X donates an impurity element. Thermochemical calculation software, FactSage (Version 5.2,

* Corresponding author at: International Research Center for Hydrogen Energy, Kyushu University, West-4, Room 628, Motooka 744, Nishi-ku, Fukuoka 819-0395, Japan. Tel.: +81 92 802 3143; fax: +81 92 802 3223.
E-mail address: sasaki@mech.kyushu-u.ac.jp (K. Sasaki).

0378-7753/$ – see front matter © 2011 Elsevier B.V. All rights reserved.
doi:10.1016/j.jpowsour.2010.09.122

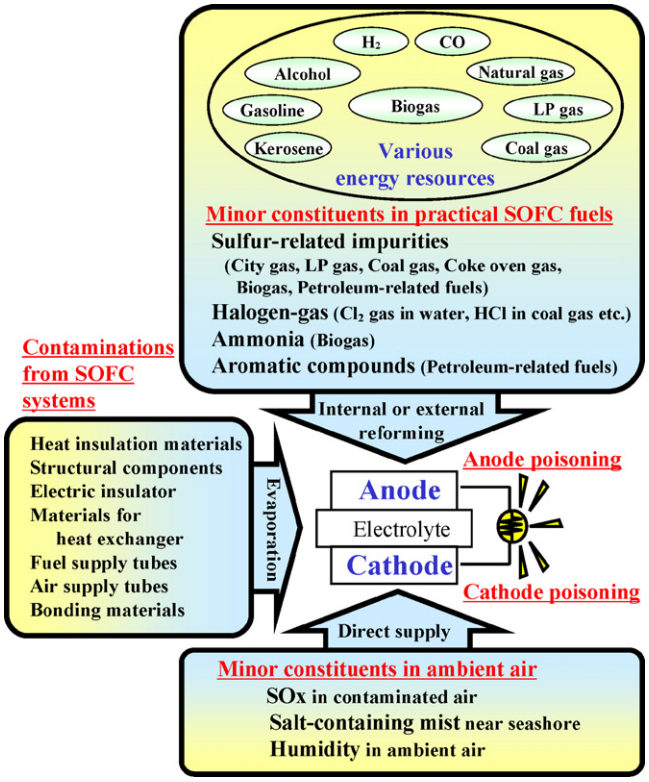

Fig. 1. Possible impurity contaminations of SOFCs.

Thermfact Ltd. (Montreal, Canada) and GTT-Technologies (Aachen, Germany)), was applied to derive the equilibrium diagrams. As examples, the C–H–O–Ni–S diagrams calculated for (a, c) 600 °C and (b, d) 800 °C are shown in Fig. 2, assuming the H_2S concentration of (a, b) 5 ppm and (c, d) 100 ppm in the fuel and the sufficient availability of Ni compared to H_2S. The diagram for 600 °C clearly shows that the stability region of Ni_3S_2(s) does exist in a hydrogen-poor region near the line connecting the positions of C, CO, CO_2, and H_2O. The stability region of Ni_3S_2 is almost disappeared at 800 °C, but Ni_3S_2 exists as the liquid state (see Fig. 2(b) and (d)). The stability region of $NiSO_4$(s) exists in the oxygen-rich region specified by the triangle connecting the positions of O_2, CO_2, and H_2O. Since fuel cell gases consist mainly of carbon, hydrogen, and oxygen, such C–H–O ternary diagrams [14] are useful to predict the chemical reactivity with impurity species for a given SOFC fuels of interest.

Thermochemical calculation was also applied to derive stability diagrams of the Ni–H–O–X (X: S, P and B) systems in a H_2-rich atmosphere (assuming $P_{H_2} \approx 1$ bar in the calculations) at 800 °C, as shown in Fig. 3(a) for the Ni–H–O–S system, in Fig. 3(b) for the Ni–H–O–P system, and in Fig. 3(c) for the Ni–H–O–B system. Fig. 3(a) clearly indicates that Ni_3S_2 can be formed only at H_2S concentrations much higher than several ppm. As shown in Fig. 3(b), phosphorus is considerably reactive to form various Ni-phosphides such as Ni_5P_2 and NiP_3, even at a very low phosphorus concentration. Fig. 3(c) indicates that Ni_4B_3(s) and NiB(s) may be stable at a high boron (HBO(g)) concentration in the reducing atmosphere at 800 °C. For the Ni–H–O–Cl system [10,16], it has been confirmed that $NiCl_2$(s) is stable even when approximately 100 ppb Cl_2 is contained in fuel gases at 800 °C, indicating that considerably low concentration of Cl_2 could affect Ni-based anodes via the formation of $NiCl_2$. Siloxanes, which might be supplied as $Si(OH)_4$(g) to anodes, were found to be decomposed to SiO_2(s), the most stable form of silicon-based compounds [10].

3. Experimental procedures for poisoning tests

Durability of SOFCs against poisoning by various impurity species has been characterized and compared using zirconia-based model cells. Electrolyte-supported cells were used in most of durability experiments, while anode-supported cells were used to study the co-poisoning phenomena with higher hydrocarbons, schematically described in Fig. 4. Thick anode substrates (ca. 0.8 mm in thickness) coated with thin electrolyte layers (ca. 30 μm in thickness) for the anode-supported model cells were obtained from Japan Fine Ceramics Co., Ltd., Japan. As an electrolyte material, Sc_2O_3-doped zirconia (ScSZ: 10 mol% Sc_2O_3–1 mol% CeO_2–89 mol% ZrO_2, Daiichi Kigenso Kagaku Kogyou, Japan) was used. The mixture of NiO and ScSZ was applied as the anode material, while the conventional La–Sr–Mn-Oxide ($(La_{0.8}Sr_{0.2})_{0.98}MnO_3$ (LSM), >99.9%, Praxair, USA) was used as the cathode material. Since the anode layer directly attached with the electrolyte acts as a functional layer for anodic reactions, the common mixing ratio, 56 wt% NiO–44 wt% ScSZ, was applied for both the electrolyte-supported cells and the anode-supported cells for the comparison. An additional anode layer (80 wt% NiO–20 wt% ScSZ), acting as a current-collecting layer, was prepared for the electrolyte-supported cells to improve in-plane electrical conductivity in the anode layers, while such additional layer is not needed for the anode-supported cells due to their sufficiently higher in-plane conductivity in the much thicker Ni-based anode layers. Electrode layers were prepared via screen-printing, followed by heat-treatment procedures. Detailed preparation procedures have been described previously [7,15,16]. Reference electrode was prepared using Pt paste and was located on the side of the electrode to which no impurity gas was supplied. Poisoning tests were carried out mainly at 800 °C under a constant current density of 0.2 A cm^{-2} for comparison. In some cases, recovery tests were also done by substituting an impurity-containing fuel to an impurity-free fuel. Typical degradation rate of the electrolyte-supported cells and the anode-supported cells was ca. 0.3%/1000 h and ca. 3%/1000 h, respectively.

4. Anode poisoning

4.1. H_2S poisoning

H_2S poisoning has been analyzed with respect to various operational conditions [5–7]. As an example, Fig. 5 shows influence of 5 ppm H_2S contaminant on the cell performance at 800 °C for 50% pre-reformed methane based fuel with the steam-to-carbon ratio (S/C) of 2.5. The anode potential (denoted as "Cell voltage (A-Re)") was measured as the voltage between the (working) anode and the Pt reference electrode on the cathode side. An initial cell voltage drop followed by a quasi steady-state cell voltage can be observed, as previously reported [5,6], associated mainly with an increase in anodic overpotential and almost constant ohmic (IR) loss, even up to 3000 h. Exactly speaking, cell voltage generally decreased up to ca. 200 h and then remained almost constant. Cell degradation rate with 5 ppm H_2S was 0.68%/1000 h and it was slightly higher than the value without H_2S of 0.3%/1000 h. This result indicates an accelerated chemical degradation during long-term operation in the presence of minor sulfur impurities.

Poisoning mechanisms by sulfur, a typical common SOFC fuel impurity, have been extensively analyzed for various fuels, including H_2, H_2–CO, CH_4, partially reformed CH_4, and simulated biogas [3–7,10]. Based on the findings and considerations mentioned below, possible sulfur poisoning mechanisms are summarized, as schematically described in Fig. 6. For relatively low concentrations (ppm level) of sulfur, reversible processes associated with adsorption/desorption of sulfur have been considered as the pre-

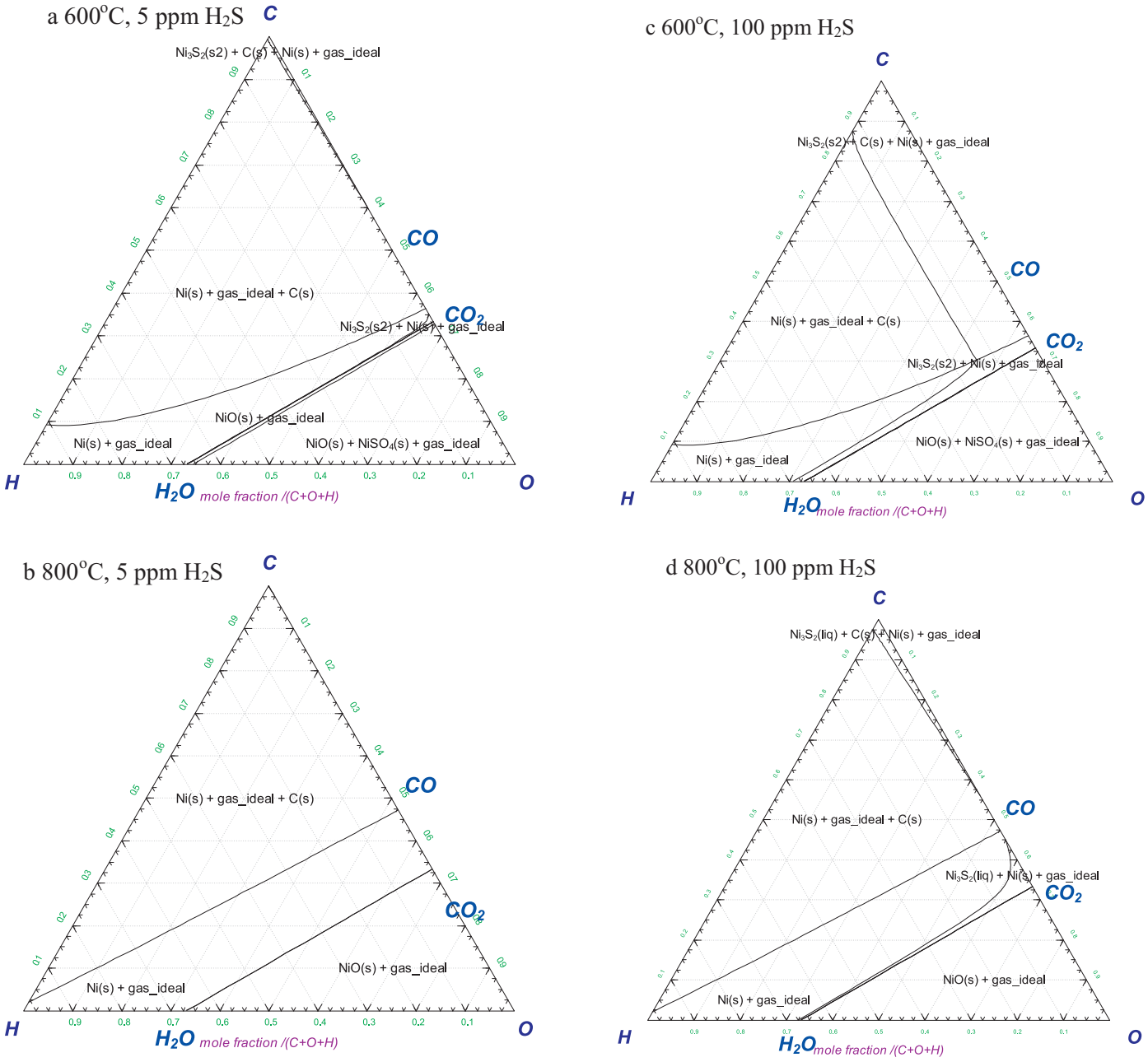

Fig. 2. C–H–O–Ni–S stability diagram showing the stable region of Ni-sulfur compounds, thermochemically calculated for (a) 600 °C and (b) 800 °C with 5 ppm H_2S and (c) 600 °C and (d) 800 °C with 100 ppm H_2S. The stability region of Ni_3S_2 locates near the line along with the positions of C, CO, CO_2, and H_2O. The stability region of $NiSO_4$ lies in the oxygen-rich triangular region surrounded by the lines among the positions of O_2, CO_2, and H_2O. Mixtures of gaseous species are denoted as "gas_ideal" in the figures, as all gaseous species have been considered as ideal gases in the thermochemical calculations.

dominant mechanism [5–7], as described in Fig. 6(b). Importance of dissociative adsorption of sulfur on Ni has been verified both experimentally [17] and theoretically [18–20]. The initial cell voltage drop remained almost constant at the fuel utilizations ranging from ca. zero to 75% [21], but increased considerably in CO-rich fuels [5,6]. As schematically shown in Fig. 6(e) and (f), larger voltage drop in CO-rich fuels (i.e. H_2-poor fuels) may be partly due to more preferred adsorption of sulfur on Ni in the equilibrium reaction ($H_2S(g) \leftrightarrows S_{ad} + H_2(g)$)) with decreasing H_2 concentration. At a higher sulfur concentration and/or a lower operational temperature, an irreversible degradation had been observed associated with the oxidation of Ni in case anodic overpotential was very large [5,6], as described in Fig. 6(g). Sulfur poisoning to internal reforming reactions is also serious as shown in Fig. 6(d) compared with Fig. 6(c), so that much larger cell voltage drop has been observed in case CH_4-rich fuels were supplied [7]. In addition, the C–H–O–Ni–S stability diagram, as shown in Fig. 2, suggests that the formation of Ni_3S_2 (melting point: 787 °C) could be possible for hydrogen-poor fuels, as described in Fig. 6(h).

4.2. Microstructural changes by other impurities

Impurity poisoning phenomena have been analyzed for other impurities, including chlorine, phosphorus, boron, and siloxane on the anode side. Fig. 7 shows FESEM micrographs of anodes poisoned by these impurities of ppm levels [10]. Chlorine poisoning was mainly associated with the sublimation of $NiCl_2$, while siloxane poisoning led to silica deposition. Phosphorus is reactive

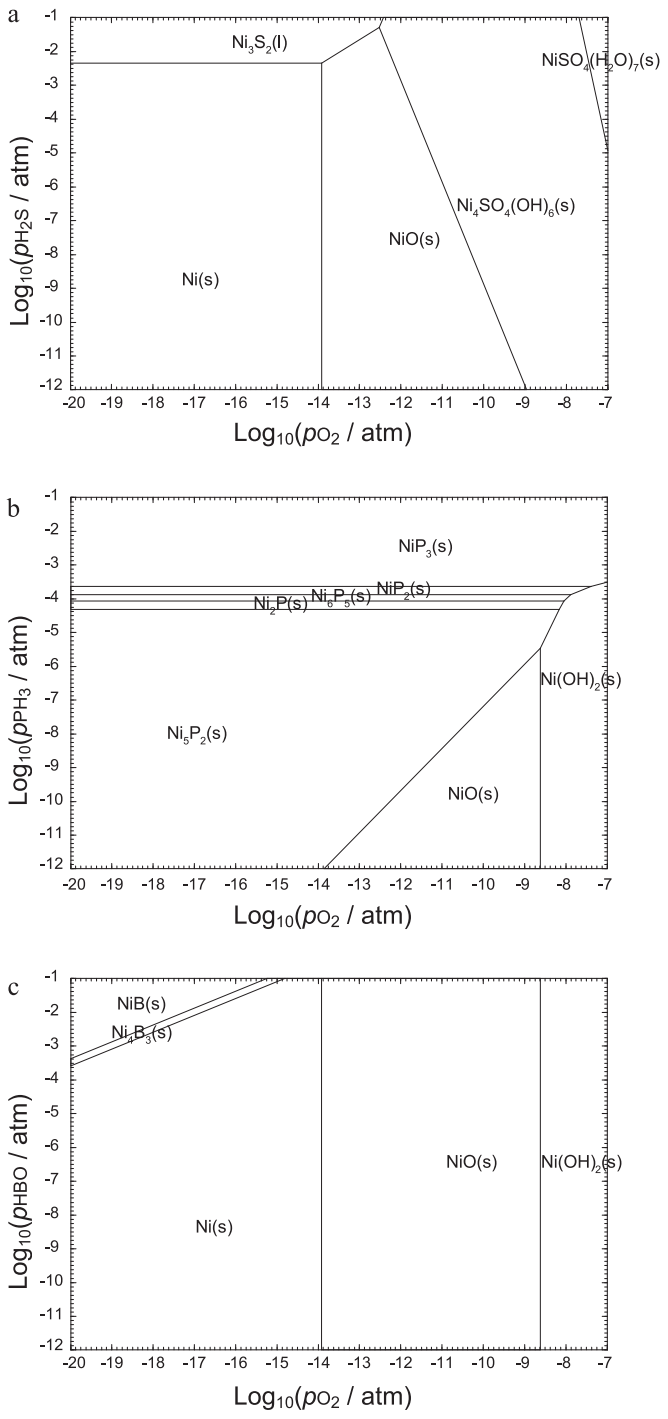

Fig. 3. Stability diagrams of the Ni–H–O–X (X: (a) S, (b) P and (c) B) system thermochemically calculated at 800 °C assuming $P_{H_2} \approx 1$ bar.

with Ni to form a eutectic compound. The presence of boron accelerated the grain growth of Ni in the anodes. In fact, a supply of real coal gas, containing various impurities such as sulfur, to SOFC anodes can lead to partially melted anode microstructure as reported, e.g. by Kuramoto et al. [22]. Similar structural change has also been observed in phosphorus poisoning reported, e.g. by Marina et al. [23].

4.3. Phosphorus and boron poisoning

Fig. 8(a) shows the cell voltage poisoned by ca. 2 ppm PH_3 for 100 h. The degradation of cell voltage was confirmed to be ca.

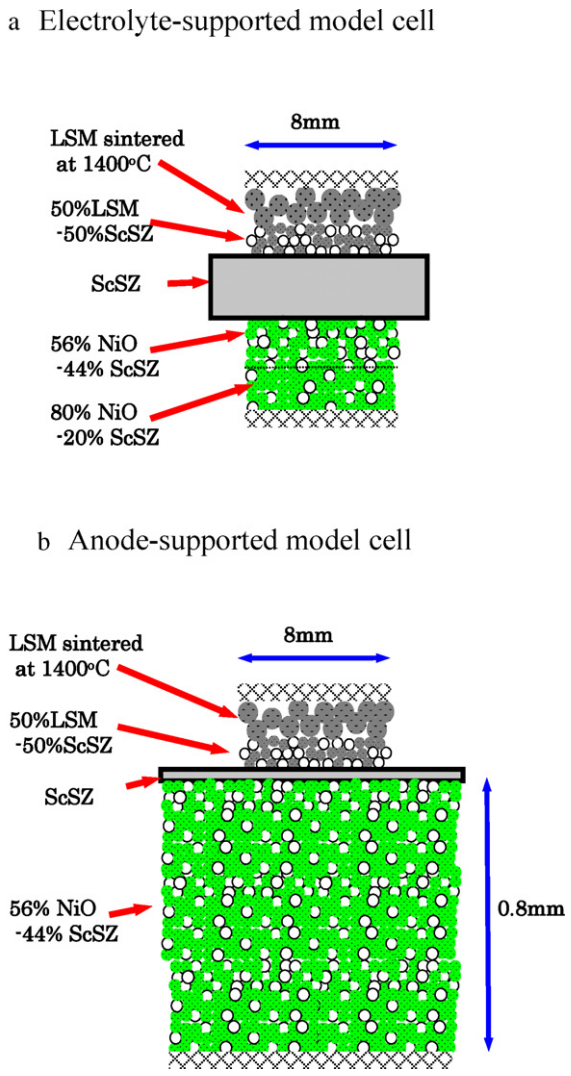

Fig. 4. Schematic drawings of SOFC model cells used in this study for systematically comparing various chemical degradation phenomena: (a) electrolyte-supported model cell and (b) anode-supported model cell.

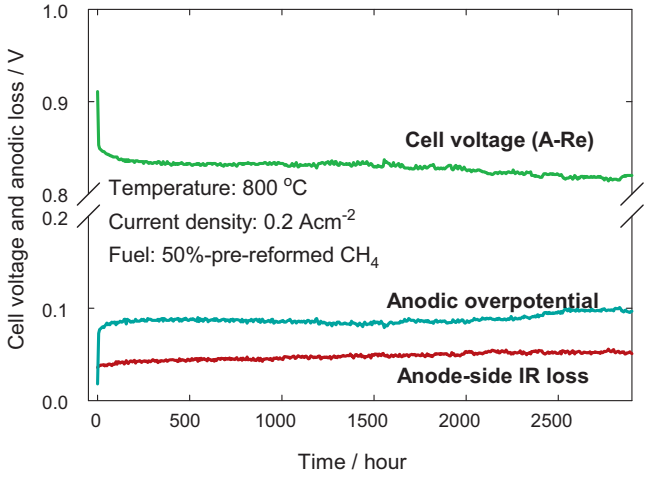

Fig. 5. Cell voltage (anode potential vs. Pt reference electrode on the cathode side), anodic overpotential, and anode-side ohmic loss, measured at 0.2 A cm^{-2} during 5 ppm H_2S poisoning at 800 °C for the 50%-prereformed CH_4 fuel with S/C = 2.5, up to 3000 h. "(A-Re)"means the cell voltage obtained between the anode and the reference electrode, so that the influence of the cathode-side voltage loss has been excluded.

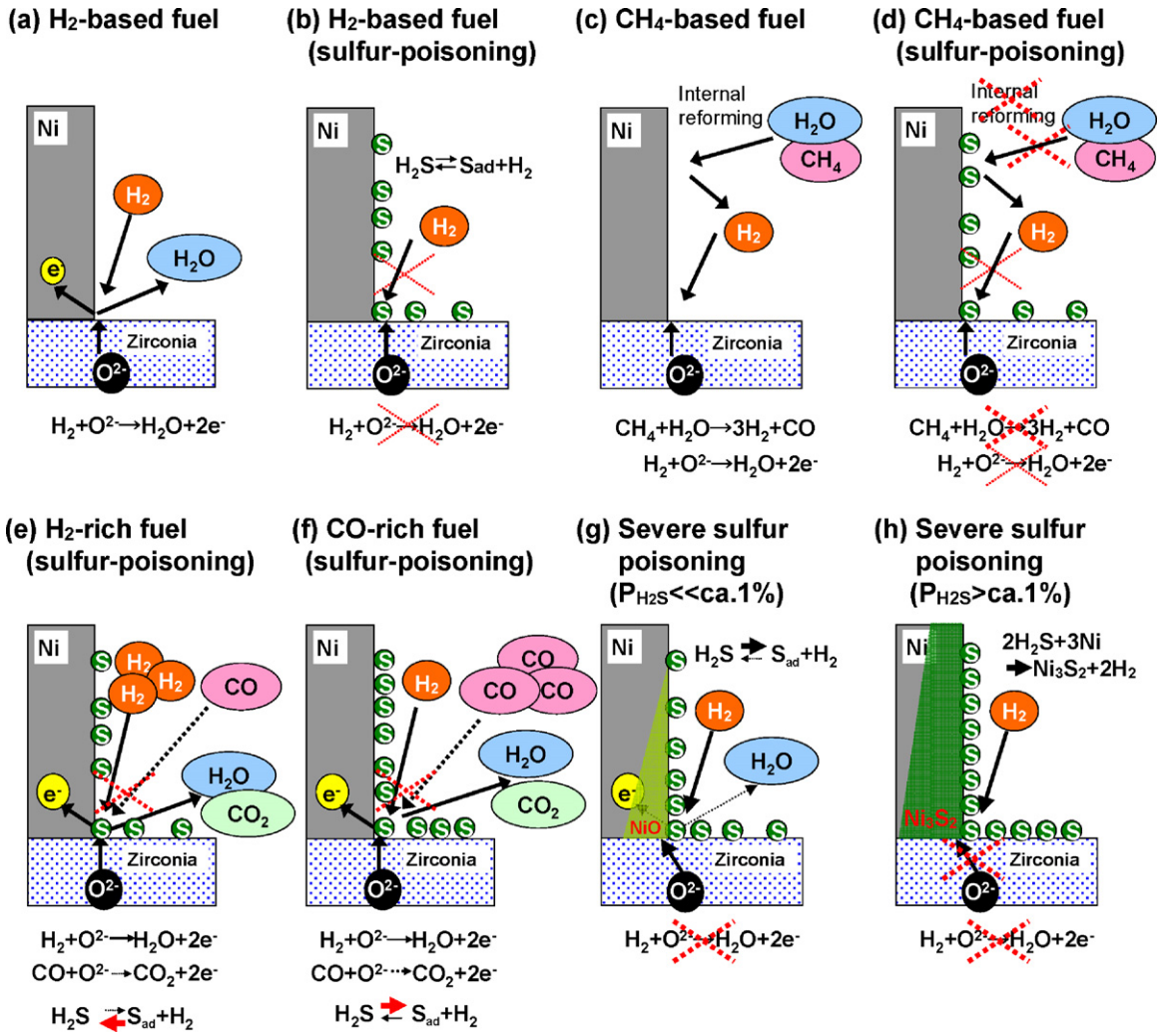

Fig. 6. Possible sulfur poisoning mechanisms of SOFCs.

18% after 100-h poisoning, which was mainly attributed to an increase in anodic overpotential at 800 °C. FESEM-EDX observation (see Fig. 7) clearly revealed that supply of phosphorus impurity resulted in the formation of melted Ni-based particles, and this occurred mostly at around the anode surface. Similar phenomena including voltage and anode microstructural change were observed in the case of boron poisoning by 200 ppb HBO(g) (see Figs. 7 and 8(b)), suggesting that boron-based compounds promoted the grain growth of Ni and led to gradual degradation of anode performance [10].

4.4. Chlorine poisoning

Cell voltage change, poisoned by Cl_2 in different concentrations ranging from 5 ppm to 1000 ppm at 800 °C for 150 h at a constant current density of 0.2 A cm^{-2}, is shown in Fig. 9 [16]. It is necessary to reveal the influence of chlorine compounds in higher concentrations on SOFC performance since 100 ppm, or higher concentration, may be contained in SOFC practical fuels, especially in coal gas. The poisoning test by up to 1000 ppm Cl_2 was therefore conducted, and durability tests at higher concentrations of Cl_2 could be regarded as "acceleration tests" of Cl_2 poisoning. As a consequence, 3%-humidified H_2 fuel containing Cl_2 at and above 100 ppm caused continuous degradation of cell voltage with an almost constant degradation rate, which increased with increasing Cl_2 concentration. The initial differences in cell voltage, ranging from 0.9 to 0.95 V, were mainly due to differences in each cell performance. The degradation rate per 100 h was ca. 9.4% for 3%-humidified H_2 fuel containing 1000 ppm Cl_2. Partial recovery of cell performance was also observed after stopping Cl_2 contamination [16].

4.5. Siloxane poisoning

Fig. 10 shows the change in cell voltages by 10 ppm siloxane (D5) in 3%-humidified H_2 at 800 °C, 900 °C, and 1000 °C [10]. This figure clearly shows that cell voltage decreased gradually with time, and at each operational temperature, poisoning by siloxane for 30–50 h resulted in a fatal degradation of cell performance. This degradation has been confirmed to be associated with the formation of SiO_2(s) in the porous cermet anodes [10], as also shown in Fig. 7. A larger amount of SiO_2 (s) was precipitated near the top surface of the anode, while a smaller amount of SiO_2 (s) was also located in the anode.

4.6. Co-poisoning by sulfur and hydrocarbons

Un-reformed hydrocarbons and sulfur could simultaneously flow into the actual SOFC systems as minor impurities, especially in case desulfurization reactor is degraded. This co-poisoning effect has been investigated experimentally. Fig. 11 shows cell voltage, in the presence of 3% C_2H_6 and 3 ppm H_2S in the 50%-prereformed methane fuel (S/C = 2.5), revealing that the voltage drop by the co-

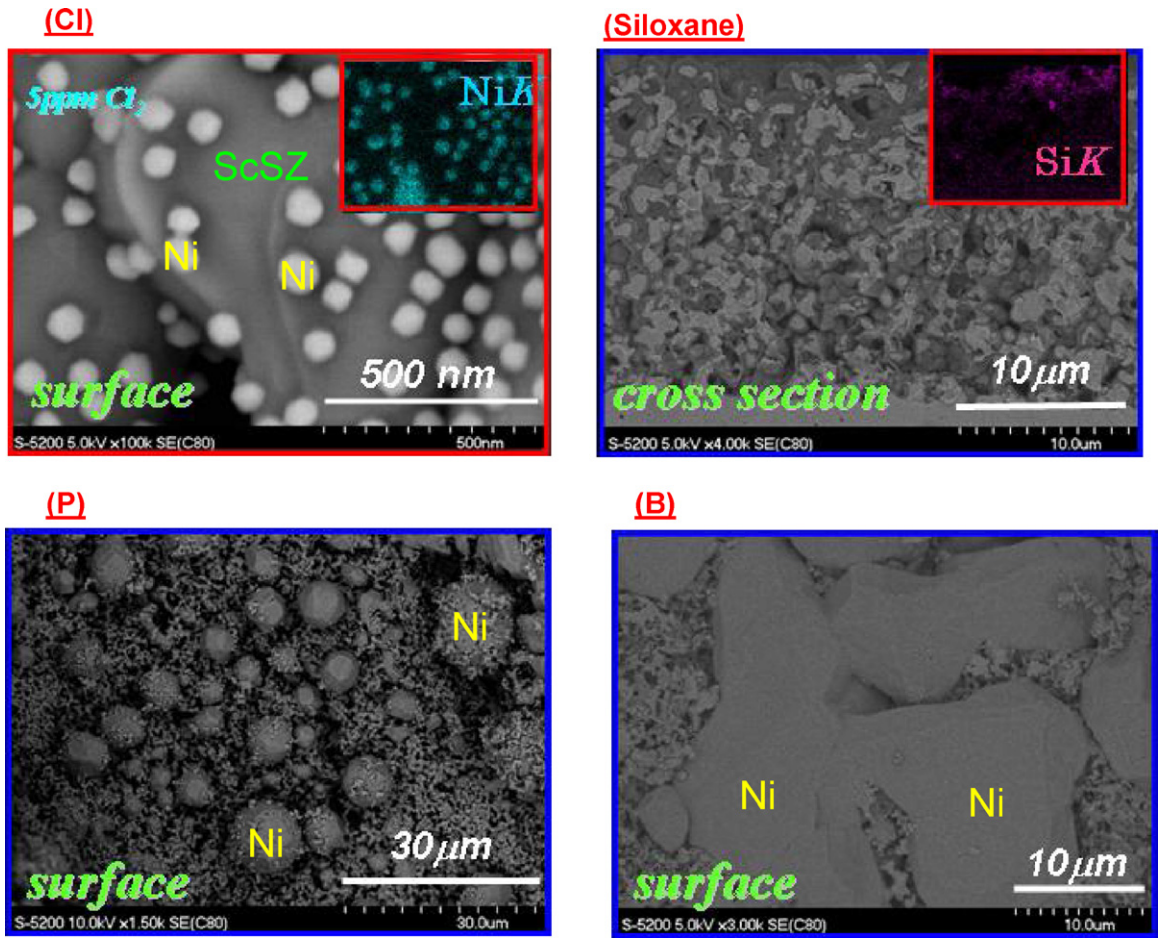

Fig. 7. Microstructural change of anodes by various impurities: Cl_2, siloxane, phosphorus, and boron [10]. Nanocrystalline Ni precipitates after chlorine poisoning, melted Ni particles after phosphorus poisoning, and grown Ni grains after boron poisoning can be distinguished, while deposited SiO_2 (dark grains) filling the porous Ni-cermet (bright grain) anode can be seen in the cross section of the anode after the siloxane poisoning.

poisoning cannot be fully recovered. As shown in Fig. 12, carbon deposition was more promoted in the presence of both a trace of H_2S and higher hydrocarbons, and considerable carbon deposition was observed especially in the presence of propane or butane, even during the operation up to 200 h. FESEM micrograph of deposited carbon shown in Fig. 13 had clearly revealed the presence of carbon nanofibers. Since gas transport is well possible among the deposited carbon nanofibers, a continuous power generation was still possible.

The co-poisoning effects have also been examined for higher hydrocarbon-based fuels containing a small amount of sulfur impurities. Fig. 14 shows the voltage and nonohmic overpotential of the whole anode-supported cells, measured at 800 °C and 40 mA cm^{-2} operated up to 5 h using iso-octane fuels humidified at S/C = 1.5, with and without H_2S impurity of 5 ppm. Optical micrographs of the anodes after these experiments are also shown in this figure. Fig. 15 shows the chemical composition of the outlet gas, measured by an automatic gas chromatograph after eliminating water vapor. Without sulfur impurity, cell voltage, nonohmic overpotential, and gas composition were stable during the experiment. However, in the presence of H_2S impurity, cell voltage gradually decreased with time, even after 3 h, associated with an increase in nonohmic overpotential. Serious carbon deposition was also observed after the measurement. In addition, as shown in Fig. 15, this performance degradation was associated with a decrease in hydrogen and CO concentrations, while concentrations of CH_4 and C_2H_4 increased with time. These results indicate the poisoning of internal reforming reactions and acceleration of carbon deposition by the minor sulfur impurity in the simultaneous presence of higher hydrocarbons.

4.7. Poisoning for anode-supported cells

Anode-supported cells are also widely used, which enable the reduction of SOFC operational temperature. Fig. 16 shows the voltage of an anode-supported cell and an electrolyte-supported cell consisting of the identical materials (see Fig. 4) as the anode functional layers, measured under the same 5 ppm H_2S poisoning condition. While an initial cell voltage drop due to the sulfur impurity was commonly observed for both types of cells followed by a meta-stable cell voltage, a certain delay time before cell voltage drop was observed for the anode-supported cells. This result indicates an importance of impurity transport within the porous anode layers from the top surface to the electrolyte/anode interface, i.e. three phase boundary.

4.8. Acceleration test procedures of impurity poisoning

Chemical degradation caused by external impurities may be accelerated with increasing impurity concentration. Therefore acceleration test procedures may be considered using fuel gases containing higher concentrations of impurity species. As a case study, Fig. 17 shows the time-dependent change of cell voltage, anode potential, ohmic loss, and anodic overpotential measured at H_2S concentration of 100 ppm, carried out as an acceleration

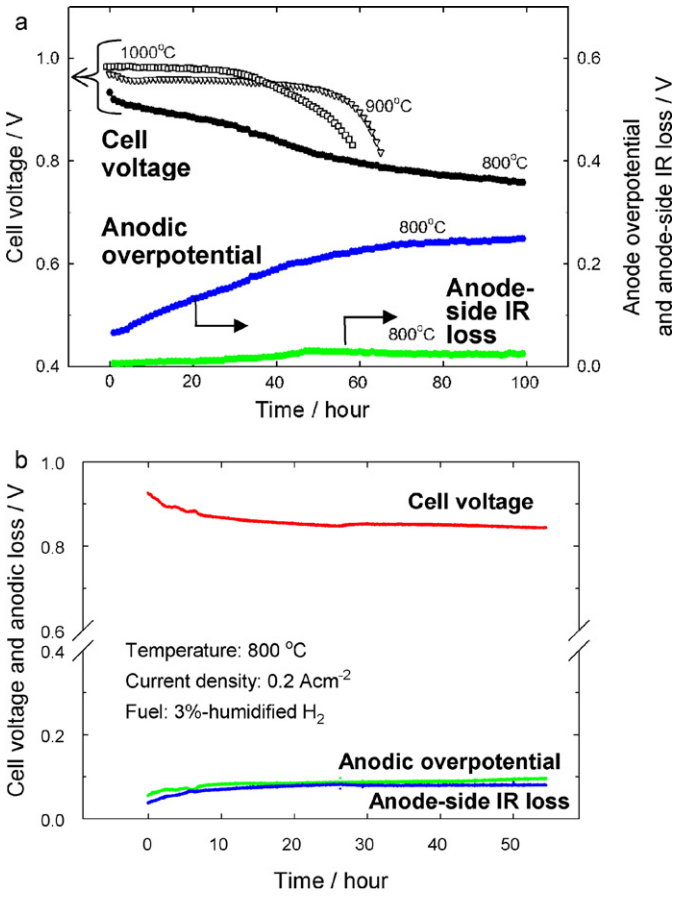

Fig. 8. Cell voltage poisoned by (a) ca. 2 ppm PH_3(g) at 800, 900, and 1000 °C, and (b) ca. 200 ppb HBO(g) at 800 °C for 100 h (fuel: 3%-humidified H_2, current density: 0.2 A cm^{-2}).

test. Since the initial cell voltage drop is a reversible equilibrium process and thus cannot be accelerated, the degradation rate in the meta-stable stage beyond ca. 200 h was evaluated. As the degradation rate tends to increase with increasing H_2S concentration, the durability tests at higher impurity concentrations may be regarded as the acceleration tests to analyze long-term durability of SOFCs, with respect to sulfur tolerance.

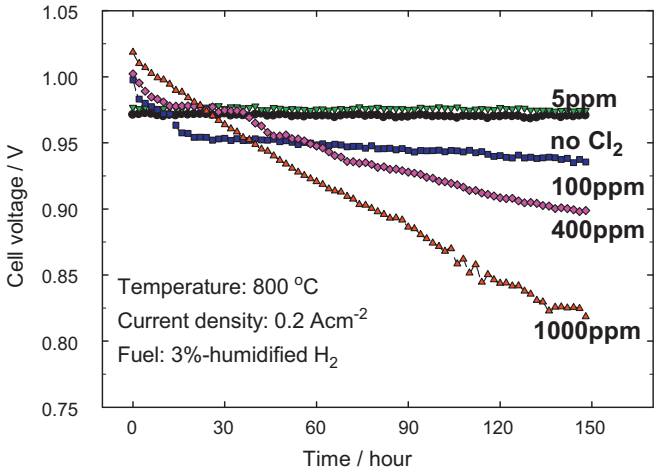

Fig. 9. Cell voltage poisoned by Cl_2 in different concentrations at 800 °C [16].

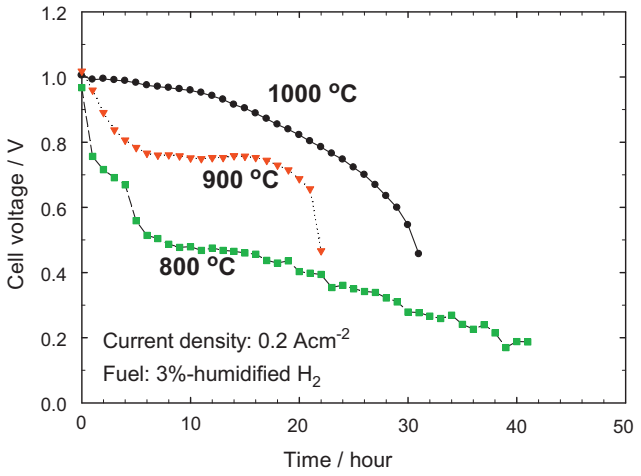

Fig. 10. Cell voltage poisoned by 10 ppm siloxane (D5) at 800 °C, 900 °C, and 1000 °C (fuel: 3%-humidified H_2, current density = 0.2 A cm^{-2}) [15].

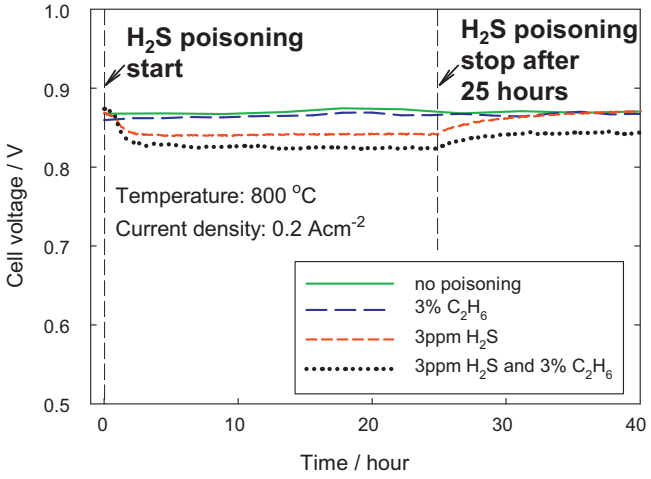

Fig. 11. Cell voltage of anode-supported SOFCs poisoned by 3 ppm H_2S for 25 h and recovered for 15 h in 50% pre-reformed CH_4 with or without 3% C_2H_6 at 800 °C.

5. Cathode poisoning

5.1. Influence of water vapor in air

Since water vapor is formed by electrochemical reactions at the anodes, the presence of water vapor is usually neglected in considering cathode performance. However, since the ambient air will be continuously supplied to the SOFC cathodes, the influence of water vapor in the ambient air should be considered in order to examine long-term practical durability of SOFC cathodes. Fig. 18 shows influence of water vapor on the performance of SOFCs with the LSM cathode. Fully humidified air contains water vapor of ca. 3%, so that the durability tests beyond 3% (H_2O) are regarded as acceleration tests [24,25]. These results demonstrated that gradual degradation was accompanied by an increase in cathodic overpotential at and below 10 vol% of water vapor (the mixture of 90 vol% air and 10 vol% water vapor). Rapid degradation occurred with an increase in cathode-side ohmic loss when 20 vol% of water vapor was supplied in the cathode gas. Under the typical operational conditions with dry, 3 and 5 vol% humidified air, nearly no degradation was distinguished.

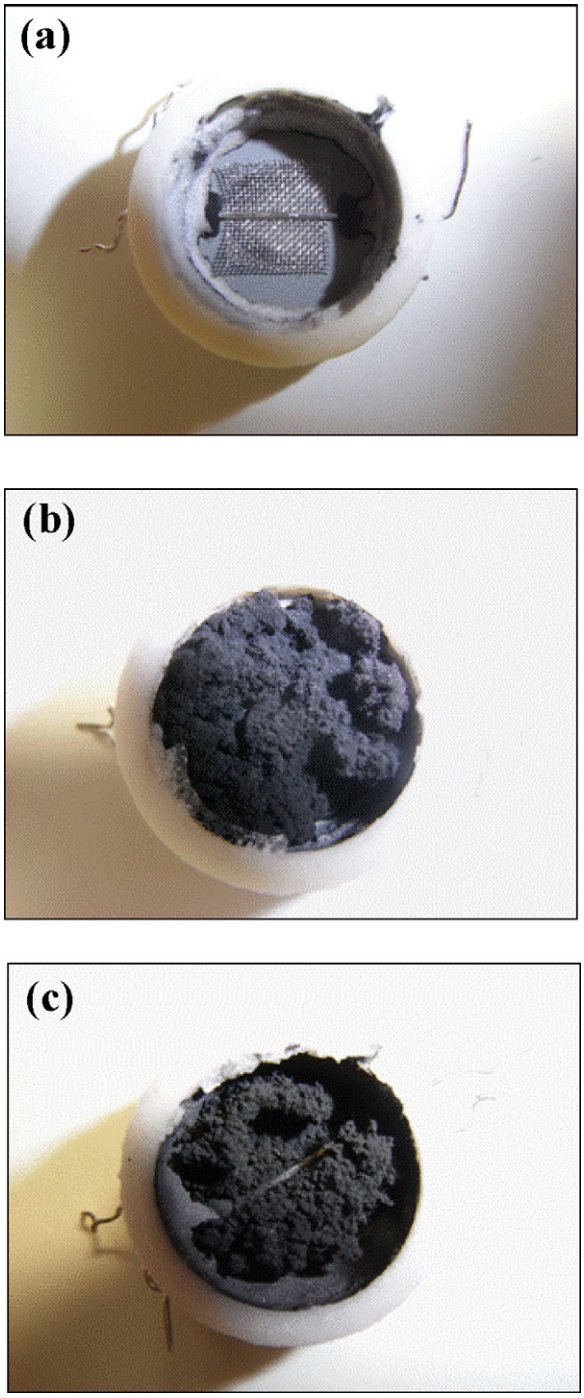

Fig. 12. Anode surface of cells after poisoning test (poisoning 200 h) by mixing with (a) 3% C_2H_6 and 3 ppm H_2S, (b) 3% C_3H_8 and 3 ppm H_2 S, and (c) i-C_4H_{10} and 3 ppm H_2S, revealing severe accelerated carbon deposition.

5.2. SO_2 poisoning

SO_2 is one of the typical contaminants in the ambient air. Chemical degradation of cathode materials has been reported to form, e.g. $SrSO_4$-related phase in acceleration experiments [24,26,27]. We are now focusing on 1000-h scale durability against SO_2 poisoning. Fig. 19 shows the dependence of cell performance on SO_2 concentration for LSM cathode up to 1000 h. While actual SO_2 concentration in atmospheric air is generally 0.1 ppm or even lower in major cities, SO_2 concentration of up to 20 ppm was mixed with air as an accelerated test to clarify the poisoning effect of sulfur on the

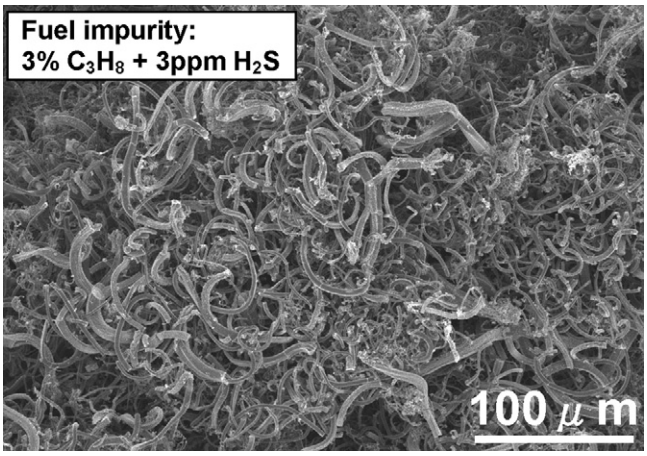

Fig. 13. FESEM image of the deposited carbon on the anode surfaces after 3 ppm H_2S poisoning test for 200 h with 3% C_3H_8.

durability of SOFC cathodes. Serious cell degradation did not occur, while a change in cell voltage has been reported at lower temperatures [28]. Cathode-side ohmic loss and cathodic overpotential did not increase over 1000 h even for 20 ppm SO_2 at 800 °C. Formation of $SrSO_4$ in the LSM cathode was detected by FESEM-EDX analysis indicating that Sr can react with SO_2 at 800 °C [24]. This chemical reaction proceeded on whole external surface of LSM.

6. Summary and outlook

Chemical degradation of SOFCs caused by various external impurities has been evaluated and compared by electrochemical characterizations, thermochemical calculations, and microstructural analysis. Fundamental knowledge with respect to degradation behaviours and poisoning mechanisms by some typical impurities has been developed that may enable the optimization of fuel purification and system components selection, and may offer acceleration test procedures. Based on the present study and the previous results cited, typical chemical degradation mechanisms are schematically summarized in Fig. 20. As described in Fig. 20(a), adsorption-type poisoning phenomena have been observed for sulfur in relatively low concentrations. In the chlorine poisoning, sublimation of $NiCl_2$(g) was predominant as shown in Fig. 20(b), while a partial recovery of cell voltage drop was also distinguished. As shown in Fig. 20(c), deposition of SiO_2(s) in the siloxane poisoning (see Section 4.5) and accelerated deposition of carbon in the simultaneous presence of sulfur and hydrocarbons (see Section 4.6) were observed. Thermochemical calculations predict in much higher sulfur concentrations the formation of Ni_3S_2, which will be in solid state at 600 °C (see Fig. 2(a) and (c)) but in liquid state at 800 °C (see Fig. 2(b) and (d)), causing reaction-type (see Fig. 20(d)) and eutectic-type (see Fig. 20(f)) poisoning phenomena, respectively. The presence of grown Ni grains in boron poisoning and melted Ni particles in phosphorus poisoning in Fig. 7 indicates irreversible chemical degradation associated with grain growth (see Fig. 20(e)) and eutectic formation (see Fig. 20(f)), respectively.

Following chemical poisoning phenomena should be taken into consideration to ensure the long-term durability of SOFCs:

(1) Reactive species with electrode materials, such as phosphorus and boron reactive with Ni, must be eliminated as much as possible.
(2) Deposition-type degradation caused by, e.g. siloxane should be prevented, which cannot be removed and recovered.
(3) Poisoning by sulfur with a typical low concentration of ppm level is reversible and can be recovered after removing sulfur

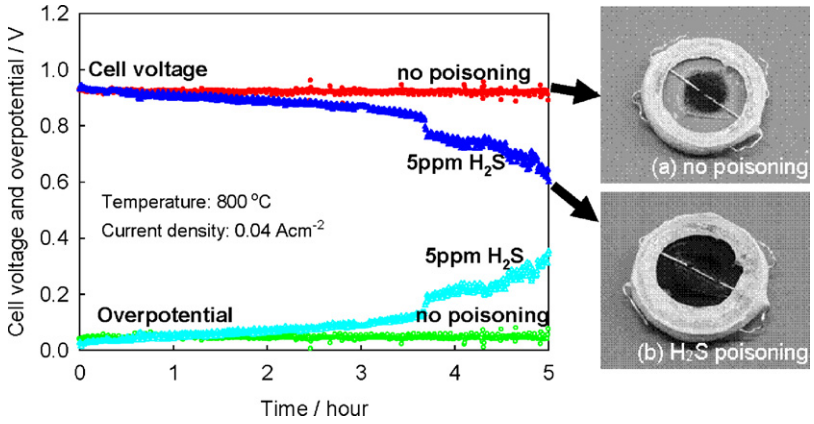

Fig. 14. Cell voltage and overpotential of anode-supported SOFCs measured in feeding iso-octane (S/C = 1.5) as a fuel at 800 °C, 40 mA cm^{-2} for 5 h: (a) no poisoning and (b) 5 ppm H_2S poisoning.

impurities. However a continuous contamination by sulfur at a high concentration can increase long-term degradation rate. Co-poisoning effects of sulfur with hydrocarbons can accelerate carbon deposition.

(4) Concentrations of moderately reactive species, such as Cl_2 for the Ni-based anodes and SO_2 for the cathodes, should be controlled below their tolerant concentrations.

Experimental studies using larger cells for practical SOFC systems are now ongoing. Further studies are being extended to understand the detail poisoning mechanisms and how the degradation behaviour is varied with changing operational parameters such as correlation between degradation rate and operational conditions including impurity concentration. Lastly, the tolerant concentra-

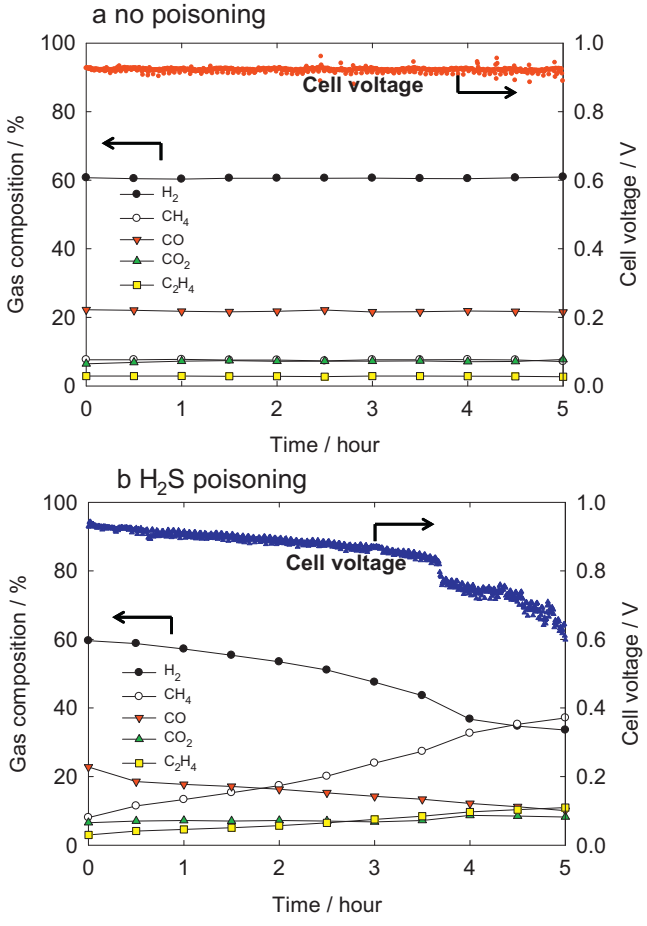

Fig. 15. Compositions of the anode exhaust gases in feeding iso-octane (S/C = 1.5) as a fuel at 800 °C, 40 mA cm^{-2} for 5 h: (a) no poisoning and (b) 5 ppm H_2S poisoning.

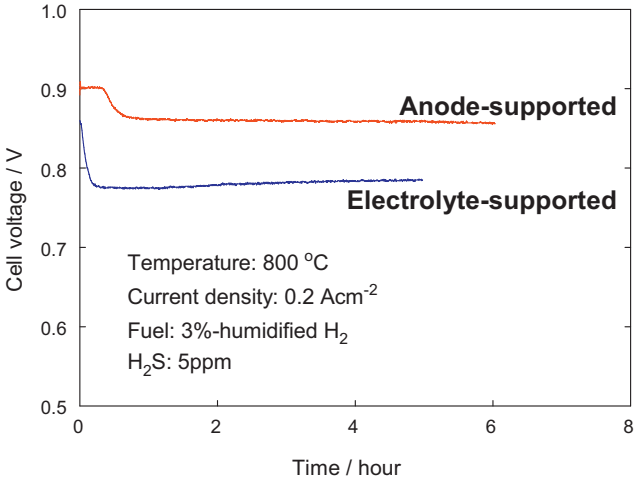

Fig. 16. Cell voltage of anode-supported SOFCs measured at 800 °C, 0.2 A cm^{-2} poisoned by H_2S (5 ppm) in for the humidified H_2-based fuel.

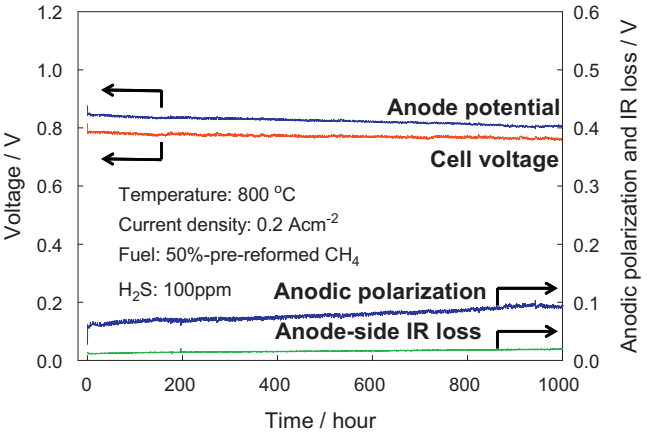

Fig. 17. Cell voltage, anodic overpotential, anode-side ohmic loss, and anode potential vs. reference electrode (Pt on the cathode side), measured at 0.2 A cm^{-2} poisoned by 100 ppm H_2S in the 50%-prereformed CH_4 fuel with S/C = 2.5 at 800 °C, up to 1000 h.

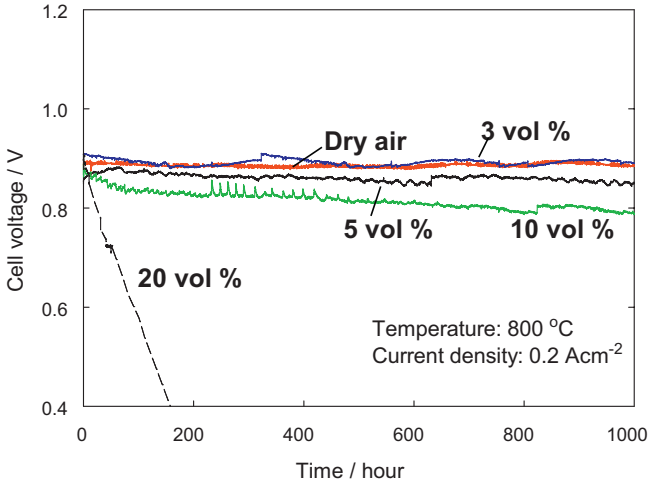

Fig. 18. Cell voltage measured at 800 °C, 0.2 A cm^{-2}, showing the influence of water vapor in air on the performance of SOFCs with the LSM cathode at different water vapor contents [17]. Volume concentration of water vapor in the water vapor–air mixtures was shown in this figure.

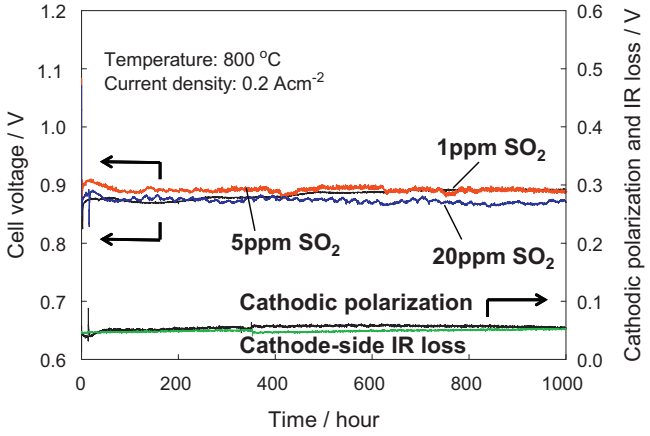

Fig. 19. Cell voltage, cathode-side ohmic loss, and cathodic overpotential measured at 800 °C, 0.2 A cm^{-2}, showing the influence of SO_2 in air on the performance of SOFCs with LSM cathodes [24].

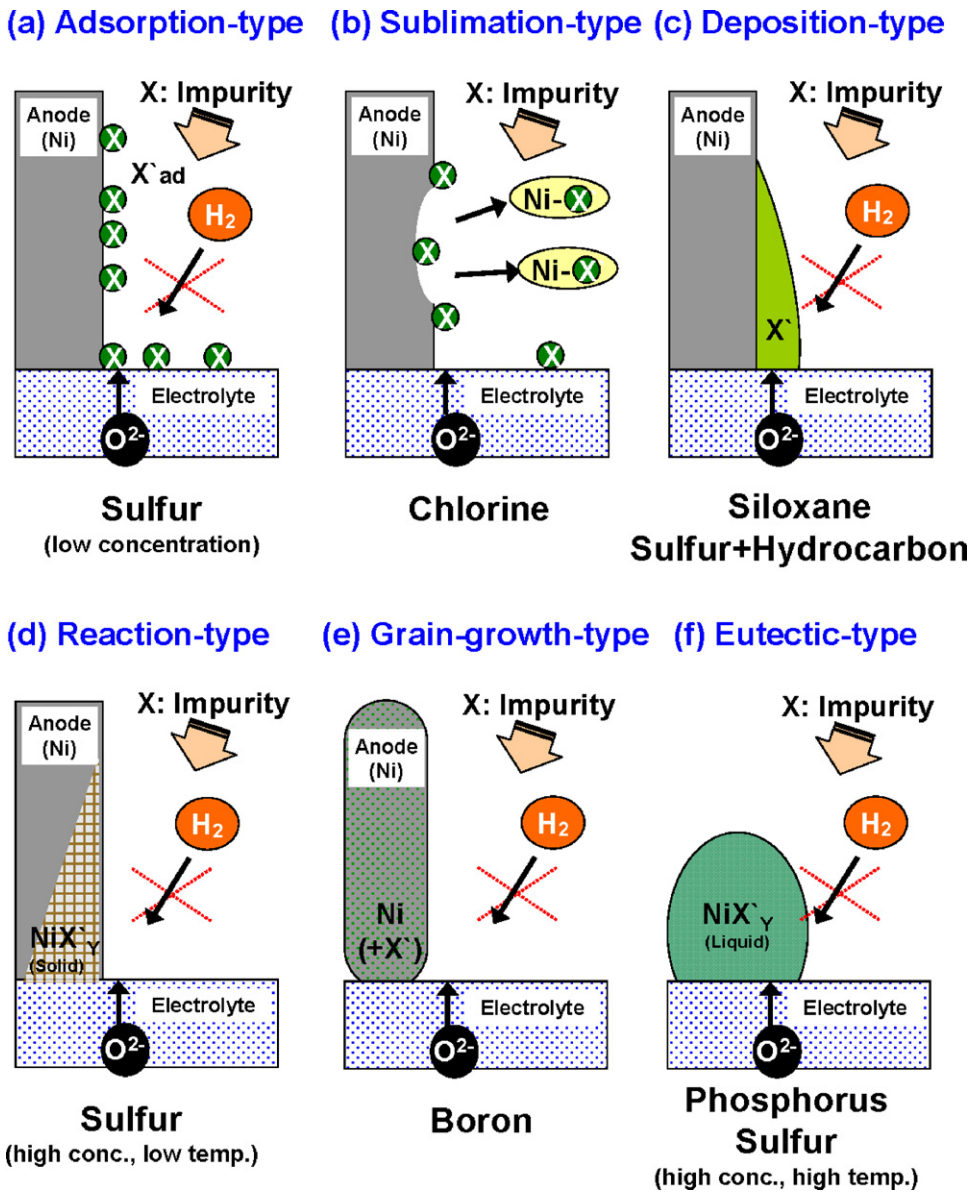

Fig. 20. Possible impurity poisoning mechanisms of SOFC anodes.

tions of each impurity to achieve sufficient durability (preferably more than 40,000 h) of SOFCs are to be revealed.

Acknowledgements

Financial support by the current NEDO project "Development of System and Elemental Technology on Solid Oxide Fuel Cells (SOFCs)" is gratefully acknowledged. We also thank Prof. H. Yokokawa of AIST and all other researchers in the current NEDO SOFC project team for helpful discussion. The support by the former NEDO project "Development of Solid Oxide Fuel Cell (SOFC) System Technology" is also appreciated, where studies on thermochemical calculations and short-term durability measurements had been made. We also thank Mr. Y. Nagai for STEM and FIB experiments, for Mr. Y. Kawazoe for co-poisoning experiments, and Profs. S. Taniguchi, Y. Tachikawa, and Y. Nojiri of Kyushu University, for reading the manuscript.

References

[1] B.C.H. Steel, A. Heinzel, Nature 414 (2001) 345.
[2] K. Sasaki, K. Watanabe, K. Shiosaki, K. Susuki, Y. Teraoka, J. Electroceram. 13 (2004) 669.
[3] Y. Matsuzaki, I. Yasuda, Solid State Ionics 132 (2000) 261.
[4] N. Komiyama, H. Sasatsu, K. Kougami, J. Iritani, 10th Symposium SOFC Society Japan Extended Abstract, SOFC Society of Japan, Tokyo, 2001, p. 59.
[5] K. Sasaki, K. Susuki, A. Iyoshi, M. Uchimura, N. Imamura, H. Kusaba, Y. Teraoka, H. Fuchino, K. Tsujimoto, Y. Uchida, N. Jingo, J. Electrochem. Soc. 153 (2006) A2023.
[6] K. Sasaki, K. Susuki, A. Iyoshi, M. Uchimura, N. Imamura, H. Kusaba, Y. Teraoka, H. Fuchino, K. Tsujimoto, Y. Uchida, N. Jingo, Proc. 9th International Symp. Solid Oxide Fuel Cells, Electrochemical Society, NJ, USA, vol. 2005-07, 2005, p. 1267.
[7] K. Sasaki, S. Adachi, K. Haga, M. Uchikawa, J. Yamamoto, A. Iyoshi, J.-T. Chou, Y. Shiratori, K. Itoh, ECS Trans. 7 (1) (2007) 1675.
[8] S. Mukerjee, K. Haltiner, R. Kerr, L. Chick, V. Sprenkle, K. Meinhardt, C. Lu, J.Y. Kim, K.S. Weil, ECS Trans. 7 (1) (2007) 59.
[9] J.F.B. Rasmussen, A. Hagen, J. Power Sources 191 (2009) 534.
[10] K. Haga, S. Adachi, Y. Shiratori, K. Itoh, K. Sasaki, Solid State Ionics 179 (27–32) (2008) 1427.
[11] F.N. Cayan, M. Zhi, S.R. Pakalapati, I. Celik, N. Wu, R. Gemmen, J. Power Sources 185 (2008) 595.
[12] H. Yokokawa, T. Watanabe, A. Ueno, K. Hoshino, ECS Trans. 7 (1) (2007) 133.
[13] K. Sasaki, J. Fuel Cell Sci. Technol. 5 (3) (2008), 031212-1.
[14] K. Sasaki, Y. Teraoka, J. Electrochem. Soc. 150 (7) (2003) A885.
[15] K. Haga, Y. Shiratori, K. Ito, K. Sasaki, ECS Trans. 25 (2) (2009) 2031.
[16] K. Haga, Y. Shiratori, K. Ito, K. Sasaki, J. Electrochem. Soc. 155 (12) (2008) B1233.
[17] J.B. Hansen, Electrochem. Solid State Lett. 11 (10) (2008) B178.
[18] J.-H. Wang, M. Liu, Electrochem. Commun. 9 (2007) 2212.
[19] D.R. Alfonso, Surf. Sci. 602 (2008) 2758.
[20] T. Ogura, T. Ishimoto, R. Nagumo, M. Koyama, Proc. 9th Europ. SOFC Forum, Chapt. 7, European Fuel Cell Forum, Lucerne Switzerland (2010) 128.
[21] T. Yoshizumi, E. Yuki, Y. Shiratori, K. Sasaki, Proc. 9th Europ. SOFC Forum, Chapt. 7, European Fuel Cell Forum, Lucerne Switzerland (2010) 77.
[22] K. Kuramoto, K. Matsuoka, Y. Suzuki, H. Kishimoto, K. Yamaji, Y.-P. Xiong, T. Horita, M.E. Brito, H. Yokokawa, ECS Trans. 25 (2) (2009) 2149.
[23] O.A. Marina, L.R. Pederson, C.A. Coyle, E.C. Thomsen, G.W. Coffey, ECS Trans. 25 (2) (2009) 2125.
[24] R.R. Liu, S.H. Kim, Y. Shiratori, T. Oshima, K. Ito, K. Sasaki, ECS Trans. 25 (2) (2009) 2859.
[25] S.H. Kim, K.B. Shim, C.S. Kim, J.-T. Chou, T. Oshima, Y. Shiratori, K. Ito, K. Sasaki, J. Fuel Cell Sci. Technol. 7 (2010), 021011-1.
[26] Y.-P. Xiong, K. Yamaji, T. Horita, H. Yokokawa, J. Akikusa, T. Inagaki, J. Electrochem. Soc. 156 (5) (2009) B588.
[27] K. Yamaji, Y. Xiong, M. Yoshinaga, H. KIshimoto, M.E. Brito, T. Horita, H. Yokokawa, J. Akikusa, M. Kuwano, ECS Trans. 25 (2) (2009) 2853.
[28] S.H. Kim, T. Ohshima, Y. Shiratori, K. Ito, K. Sasaki, Mater. Res. Soc. Symp. Proc. 1041 (2008) 131.